

Structure and Properties of Conductive Polyaniline Blends

Dr.Sarika A. Khapre, S.P. Yawale and S.S. Yawale

Department of Physics, GENBA SOPANRAO MOZE COLLEGE OF ENGINEERING

BALEWADI, PUNE-45

Vidarbha Institute of Science and Humanities, Amravati 444 604 Maharashtra (India)

Email:sakhapre@yahoo.com

I. Introduction

Conducting polymers:Polymers are a large class of materials consisting of many small molecules called monomers, that can be linked together to form long chains thus, they are known as macromolecules. A typical polymer may include tens of thousands of monomers. Because of their large size, polymers are classified as macrom.

The field of conducting polymers becomes one of the most promising fields of research and development. These polymers have tremendous applications in different fields, especially in the electronics industry. However, the major concern in this area is the lack of processibility of these polymers. Nowadays, the rapidly expanding field of nano conducting a polymer composite is generating many exciting new materials with novel properties.

Most commercially produced organic polymers are electrical insulators. Conductive polymers, which are almost always organic, have extended delocalized bonds (often comprised of aromatic units) that creates a band structure similar to silicon, but with localized states. When charge carriers (from the addition or removal of electrons) are introduced into the conduction or valence bands the electrical conductivity increases dramatically. Technically almost all known conductive polymers are semiconductors due to the band structure, however so-called zero band gap conductive polymers may behave like metal. The most notable difference between conductive polymers and inorganic semiconductors is the mobility which, until very recently, was dramatically lower in conductive polymers than their inorganic counterparts, though recent advancements in self-assembly are closing that gap.

Until about 30 years ago all carbon based polymers were rigidly regarded as insulators. The idea that plastics could be made to conduct electricity would have been considered to be absurd. Indeed, plastics have been extensively used by the electronics industry because of this very property. They were utilized as inactive packaging and insulating material.

This very narrow perspective is rapidly changing as a new class of polymer known as intrinsically conductive polymer or electroactive polymers are being discovered. Although this class is in its infancy, much like the plastic industry was in the 30's and 50's, the potential uses of these are quite significant. At the start of the 60's the research priorities at the Plastics Research Laboratory of BASF in Ludwigshafen, Germany centered on postulating new structural properties of polymers made by oxidative coupling. Copper chloride and aluminum chloride were used to make an oligobenzene from benzene. This reaction was extended to include other aromatic compounds and heterocycles. These reaction products were characterized in terms of thermoelectric power and photo- and dark conductivities. To their surprise polyphenylene and polythiophene showed electrical conductivities of up to 0.1 S cm^{-1} . Not only this was the highest value yet obtained, but it was the first capable of conducting electricity

The Polyaniline-PEO blend doped with lithium salt is prepared. In this series Polyaniline -PEO blend doped with lithium sulphate and the properties of the composite film such as dc conductivity, Impedance spectroscopy, Transference Number, TG/DTA, FTIR, SEM etc. are studied. The results so obtained are presented and discussed below.

Keywords: Polyaniline, Polyethylene oxide, Li_2SO_4

II. MATERIAL AND METHOD

The aniline monomer was A.R. grade reagent obtained from M/S S.D. Fine Chem. (India), the chemical ammonium persulfate $[(\text{NH}_4)_2\text{S}_2\text{O}_8]$ was received from M/S Loba Chemie India and was used as such. The concentrated hydrochloric acid was obtained from M/S S.D. Fine Chem. (India). PEO (polyethylene oxide) was received from Merck company. Solvents NMP (1-methyl 2-pyrrolidone), distilled water and methanol were used after purification,

Li₂SO₄.H₂O were received from M/S LobaChemie India and ware used as such.

III. EXPERIMENTAL

A. PREPARATION OF SAMPLE

Polyaniline was synthesized in conventional route in aqueous medium using mineral acid such as HCl as dopant ion and oxidizing agent ammonium persulfate, (NH₄)₂S₂O₈, as initiator. Aniline monomer, acid dopant and oxidizing agent were taken in the molecular ratio of 1:1:1.1. Hydrochloric acid was taken in distilled water in which aniline monomer was added and stirred to get aniline-acid complex and kept in the freezing mixture to attain the reaction temperature of 0 - 5 °C. In another beaker, (NH₄)₂S₂O₈ was dissolved in distilled water and kept in the

freezing mixture. After both of these solutions attained the reaction temperature, they were mixed together and stirred well and kept for six hours for the completion of reaction. Polyaniline powder formed was filtered, washed thoroughly with water to remove excess salts and dried under the vacuum (10⁻³ torr) for 24 hrs to make it moisture free. [1] PANi- Li₂SO₄-PEO, were added to NMP (1-methyl 2-pyrrolidone) which was stirred for 30 min [2]. Films containing PANi- Li₂SO₄-PEO, were obtained by drying the mixtures at 75⁰C for 24 h. Film was deposited on Teflon sheet ,so that it is easy for removing the film Different percentage of composite film have been prepared such as 3 ,5,7,9,11wt % .In these films the concentration of Li-salt is varied and PANi and PEO is kept constant. The nomenclature and stiochiometry is

Table 3.1: Nomenclature and stiochiometry of the films.

wt % of Li-salt in PANi-PEO blend	Polyaniline(PAni) wt (%)	Polyethylene oxide (PEO) wt (%)	Li-salt (Li ₂ SO ₄) wt (%)
3	0.1879	1.9	0.064574
5	0.1879	1.9	0.109889
7	0.1879	1.9	0.157154
9	0.1879	1.9	0.206496
11	0.1879	1.9	0.26398

IV. RESULT AND DISCUSSION

A. Scanning Electron Microscopy images (SEM/EDAX):

The surface morphology of PANi-PEO- Li₂SO₄ blend film was examined by Scanning Electron Microscope (SEM). Fig.4.1 (a-c) illustrate the SEM image PANi-PEO- Li₂SO₄ blend samples of 5, 7 and 9wt% shows that the

surface of the film(c) is smooth as compared to (a) and (b). Film (a) and (b) shows some cracks on the surface, “sponge-like” appearance observed for the 9 wt% film, indicative of a highly inhomogeneous microstructure within the composite [3] .Nature of all films is amorphous

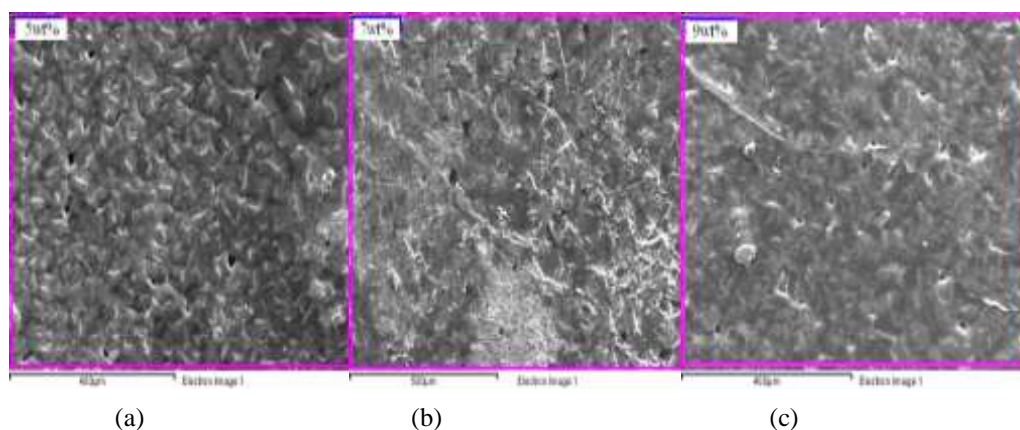
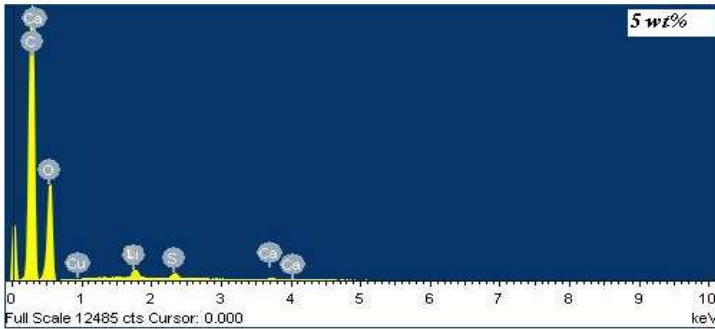


Fig.4.1 (a-c): Scanning electron micrographs of 3wt%, 7wt% and 11wt% Li₂SO₄ (PANi-PEO- Li₂SO₄) blend.

The elemental composition of PANi-PEO- Li_2SO_4 blend samples of is also determined using SEM energy dispersive analytical -X-ray (EDAX) spectroscopy. The quantitative analysis for energy dispersive X-ray analysis (EDAX) was performed for Li and S on various samples at different points. The average ratio of atomic percentage of Li: S shows that the samples have S deficiency. The existence of

lithium in the composite film is confirmed by EDAX analysis fig 4.2. A signal corresponding to sulfur also appears on the spectrum. The results of EDAX investigations highlighted are summarized in Table 4.1(a), (b),(c) for 5,7and9wt% Li_2SO_4 (PANi-PEO- Li_2SO_4) respectively. The element (%) and atomic (%) of the Li_2SO_4 (PANi-PEO- Li_2SO_4) blend are shown in table 4.6(a-c).

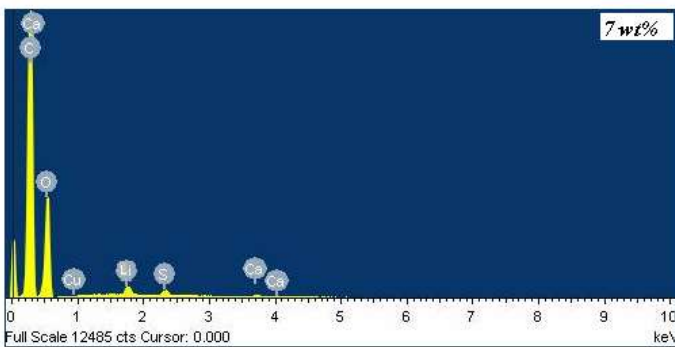
Table 4.7(a)



(a)

Element	Weight%	Atomic%
C	57.75	64.95
O	40.92	34.55
Li	0.48	0.23
S	0.35	0.15
Ca	0.14	0.05
Cu	0.36	0.08

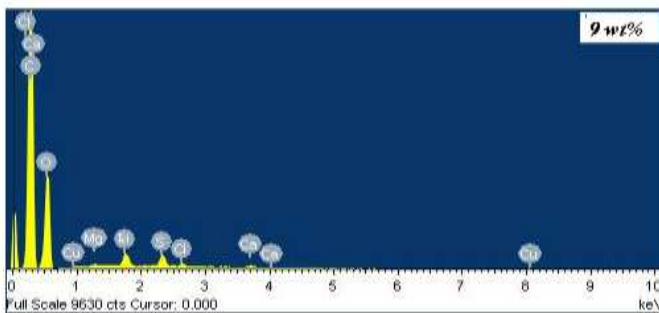
Table 4.1 (b)



(b)

Element	Weight%	Atomic%
C	58.59	65.88
O	39.55	33.38
Li	0.64	0.31
S	0.73	0.31
Ca	0.19	0.06
Cu	0.31	0.07

Table 4.1 (c)



(c)

Element	Weight%	Atomic%
C	57.6	65.06
O	40.08	33.99
Mg	0.15	0.08
Li	0.72	0.35
S	0.74	0.31
Cl	0.24	0.09
Ca	0.17	0.06
Cu	0.3	0.06

Fig.4.2: EDAX spectra of 5, 7 and 9wt% Li_2SO_4 (PANi-PEO- Li_2SO_4) blend.

B. Fourier transforms infrared spectroscopy (FTIR) analysis :

In order to find the nature of bonding in the film material we studied FTIR spectrum of PANi-PEO - Li_2SO_4 blend. Fig (4.3)the strongest lines appear at 1037 cm^{-1} and 640.37 cm^{-1} of 5and 7wt% respectively which correspond to the (SO_4) and (SO_4) of the sulphate respectively [4]. The peak 486.9 cm^{-1} of 9wt% and 1138 cm^{-1} of 5wt% vibrations of

Li_2SO_4 . several translational modes of Li^+ ion can be connected due to their presence in the region of $400\text{--}450\text{ cm}^{-1}$ of 7wt% [5]

In polyaniline polarons are responsible for the broad absorption band at wave numbers above $3431.36.8\text{ cm}^{-1}$ of 7wt% and 2929.87 cm^{-1} of 9wt% [6, 7, 8]. The absorption band at 1274.95 cm^{-1} of 5wt% is due to C-N stretching of secondary aromatic amine which represents π

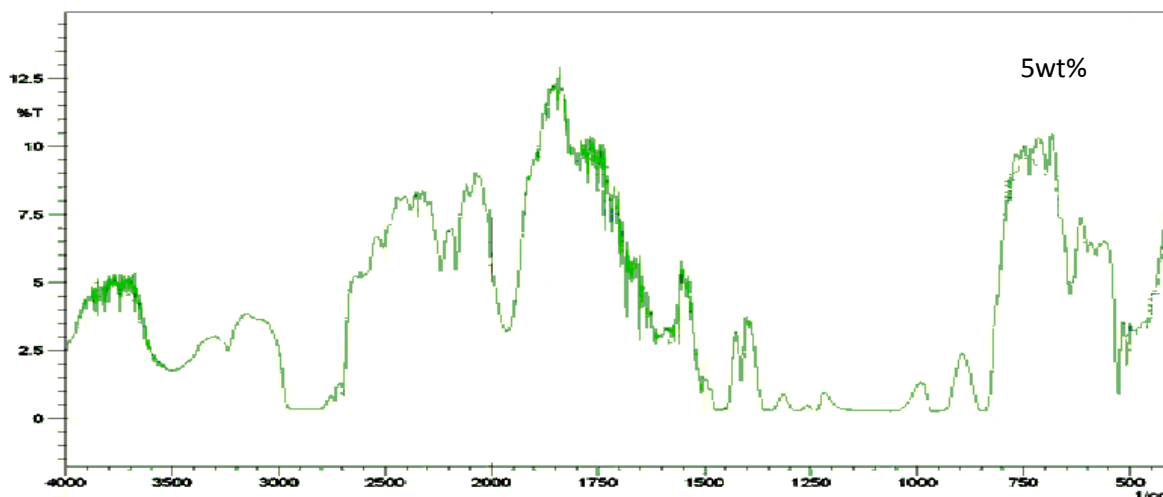
electron delocalization induced in the polymer by protonation [6]. The band characteristic of the conducting protonated form is observed at about 12334.44 cm^{-1} of 5wt% which has been interpreted as $\text{C-N}^+\bullet$ stretching vibration in the polaron structure [9]. The region $900\text{--}700\text{ cm}^{-1}$ corresponds to aromatic ring and out-of-plane C-H deformation vibrations. Their frequencies are mainly determined by the number of adjacent hydrogen atoms in the

ring [10]. Also peak 1581.63 cm^{-1} , 1355.96 cm^{-1} of 5wt% ,these peaks are corresponding to most of the characteristic peaks for PEO exhibit a large broad band of asymmetric CH_2 stretching between 2843.0 cm^{-1} and narrow band of lower intensity at 2740 cm^{-1} of 9wt% [11].

Table 4.2 shows the Peak position for 5, 7 and 9wt% Li_2SO_4 (PAni-PEO- Li_2SO_4) blend.

Table 4.2: Peak position for 5, 7 and 9wt% of Li_2SO_4 (PAni-PEO- Li_2SO_4) blend

Sr.No.	Peak position cm^{-1}		
	5% Li_2SO_4 (PAni-PEO- Li_2SO_4)	7% Li_2SO_4 (PAni-PEO- Li_2SO_4)	9% Li_2SO_4 (PAni-PEO- Li_2SO_4)
1	401.19	401.19	-
2	424.34	420.48	-
3	435.91	443.63	-
4	447.49	474.49	486.06
5	694.37	640.37	-
6	727.16	-	727.16
7	738.74	-	738.74
8	759.95	-	759.95
9	839.3	-	837.11
10	933.55	-	856.39
11	941.26	-	939.33
12	952.84	-	-
13	1037.7	-	1037.7
14	1138	1130.29	-
15	1234.44	1230.58	1234.44
16	1274.95	-	-
17	1355.96	1359.82	1359.82
18	1581.63	1533.41	1558.48
19	2740.85	2740.85	2740.85
20	2825.87	-	2843.07
21	2902.87	-	2929.87
22	3415.93	3431.36	3437.15



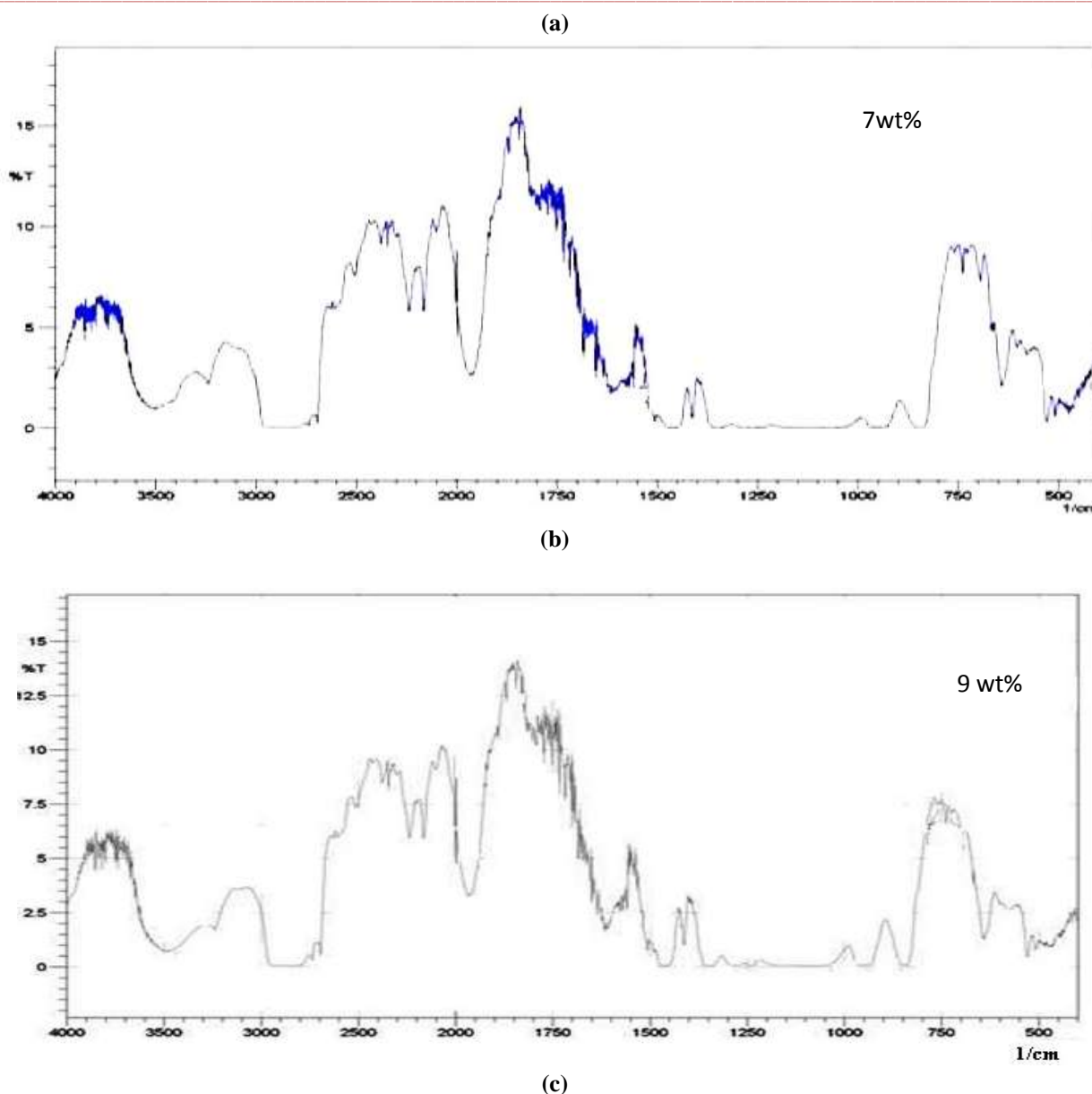


Fig 4.3: FTIR spectra for a) 5wt% b) 7wt% c) 9wt% of Li_2SO_4 (PAni-PEO- Li_2SO_4) blend

C. Thermogravimetry (TG) / Differential thermal analysis (DTA):

Thermo gravimetric analysis was carried out for various polymers to determine the weight loss at different temperatures. Thermal stability of the PAni-PEO- Li_2SO_4 blend was assessed from analysis of the TG and DTA curves Fig. 4.4(a-c). The main data are summarized in Table 4.3

In (Fig. 4.4a) the film demonstrated one step degradation, it was in the temperature range of 255to 435°C. One endothermic event and two exothermic events are observed in the PAni-PEO- Li_2SO_4 thermograms (Fig. 4.4a). The first event occurs at 68.91°C temperature, it is called as glass transition temperature because at this temperature there is transition from a disordered solid to a liquid. The first event

is accompanied by a 4.3% weight loss and is related to the removal of the physically adsorbed water. Two exothermic events occur at 325.62°C and 446.23°C. These two events is accompanied 84.145% and 6.577% weight loss.

In (Fig. 4.4 b) the film demonstrated one step degradation. It was in the temperature range of 255to 425°C. One endothermic event and four exothermic events are observed in the PAni-PEO- Li_2SO_4 thermograms. The first event occurs at 69.13°C temperature, it is called as glass transition temperature. The first event is accompanied by a 5.39% weight loss and is related to the removal of the physically adsorbed water. Three exothermic events occur at 244.12 °C, 297.84 °C, 373.36 °C, 452.34 °C and .These four events are accompanied by 85.905% and 5.307% weight loss.

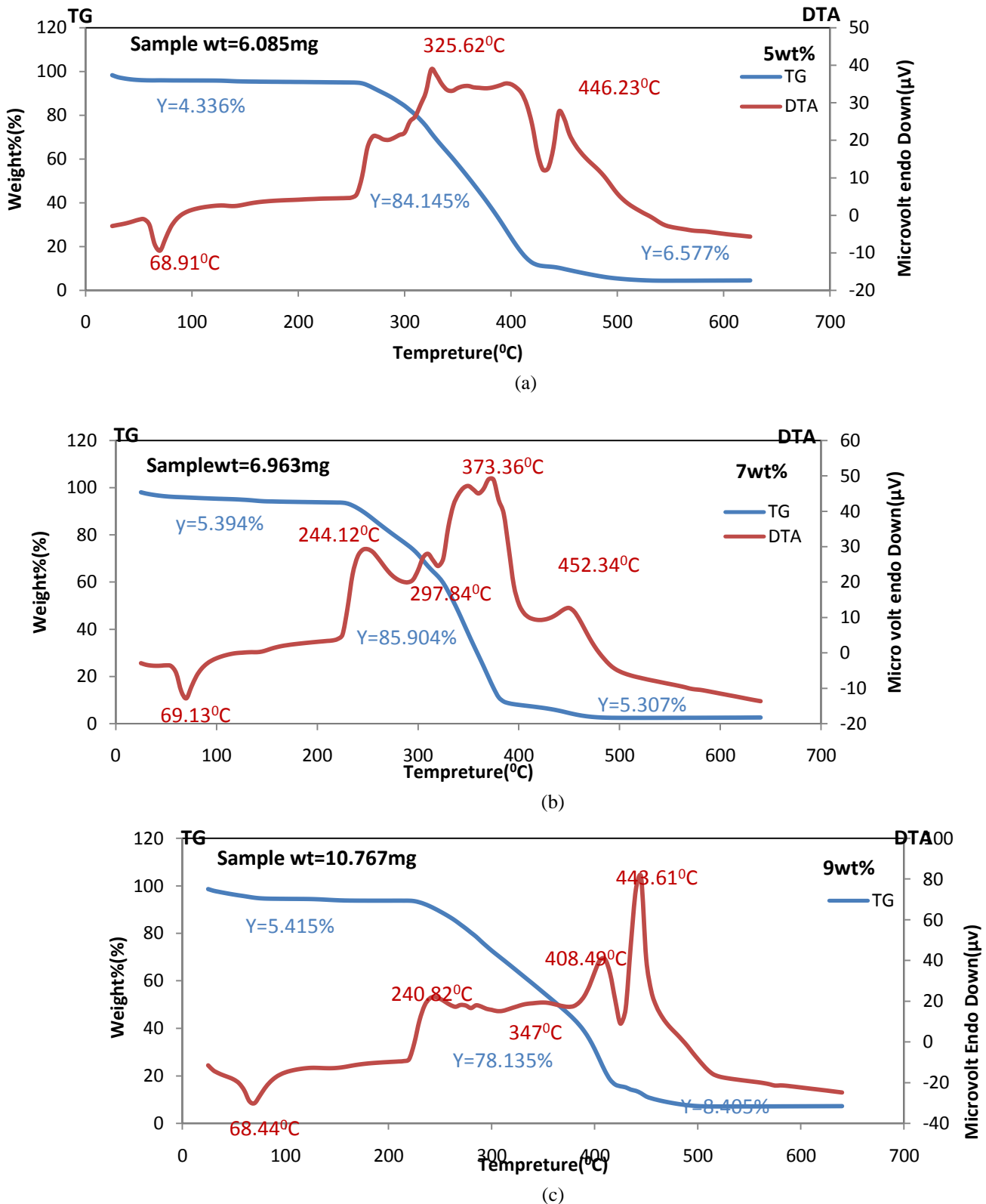


Fig 4.4: TG/DTA curves of a) 5wt% b) 7wt% c) 9wt% of Li_2SO_4 (PAni-PEO- Li_2SO_4) blend.

In (Fig. 4.4 c) the film demonstrated one step degradation. It was in the temperature range of 250 to 460°C. One endothermic event and four exothermic events are observed in the PAni-PEO- Li_2SO_4 thermograms. The first event occurs at 68.44°C temperature, it is called as glass transition temperature. The first event is accompanied

by a 5.415% weight loss and is related to the removal of the physically adsorbed water. Four exothermic events occur at 240.82 °C, 347 °C, 408.49 °C and 443.61 °C. These Four events is accompanied 78.135% and 8.4057% weight loss.

Table 4.3: TG /DTA data for PANi-PEO- Li₂SO₄ blend samples.

Sample	Peak I (Glass transition) Endothermic events		Peak II Exothermic events		Peak III Exothermic events		Peak IV Exothermic events		Peak V Exothermic events	
	T _{max} (°C)	Peak Height (μV)	T _{max} (°C)	Peak Height (μV)	T _{max} (°C)	Peak Height (μV)	T _{max} (°C)	Peak Height (μV)	T _{max} (°C)	Peak Height (μV)
5	68.98	-9.355	325.62	31.371	446.57	17.702	-	-	-	-
7	69.13	-10.067	244.12	19.988	307.62	6.239	373.36	32.556	452.34	8.028
9	68.44	-13.182	240.82	24.91	347	2.876	408.49	28.846	443.61	79.8

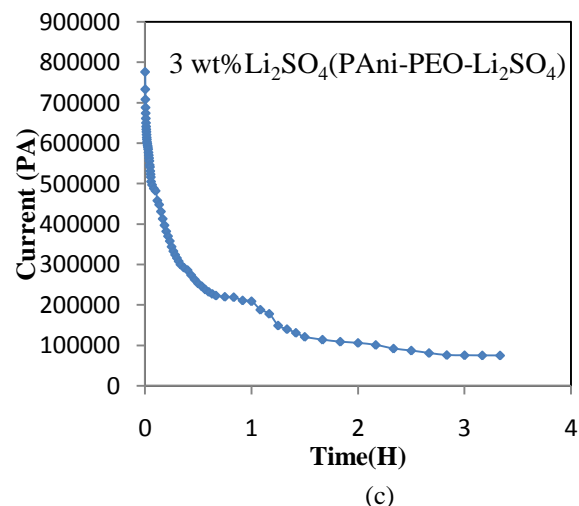
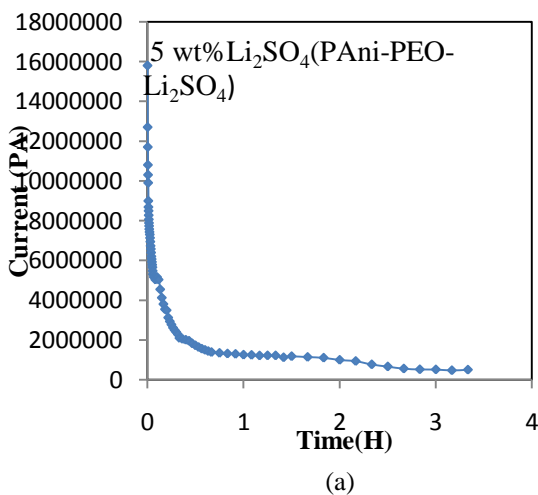
D. Transference number measurement:

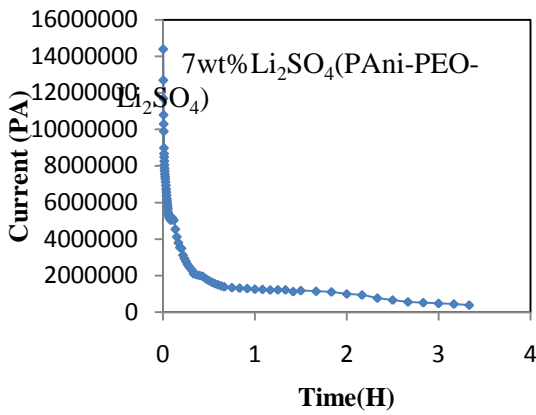
The ionic transference number was measured for all wt % of Li₂SO₄ for Pani-PEO- Li₂SO₄ blend by Wagner's polarization technique using blocking electrodes .Figure 4.5(a-e) shows variation of current as a function of time. The total current consists of both ionic current (*t_{ion}*) and electronic current (*i_e*). The ionic transference number was obtaining by using standard formula [12]

$$t_{ion} = (i_t - i_e) / i_t \tag{4.5}$$

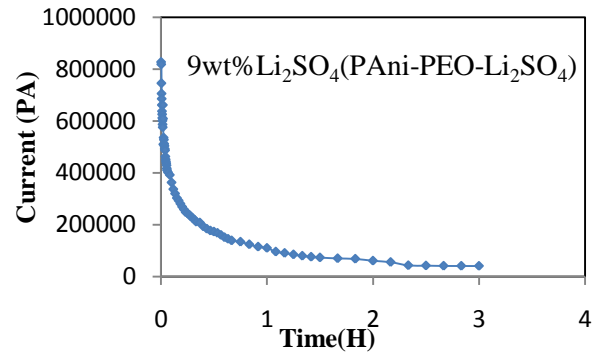
From figure 4.5 it has been observed that at initial time period all samples shows maximum current (*i_{total}*) and it start decreasing with increase in time and then it gets saturated. This maximum current (*i_{total}*) at the initial stage and higher conductivity which is already reported in dc conductivity.

is due to the flow of both electrons and ions. The exponential decrease in current with time may be due to pile up of the ions at the silver electrode (because of its blocking nature) because of the applied dc potential. Hence the saturated current is only due to the flow of electrons. Ionic transference numbers for all samples were found to be in the range of 0.903 to 0.974 from observations it is clear that PANi-PEO- Li₂SO₄ blend shows the ionic conduction. The calculated values of *t_{ion}* for different composite films are listed in Table 4.4. From the table, it is apparent that ionic transference no increases and then decreases after 7 wt% of Li₂SO₄ i.e. 7wt% of Li₂SO₄ have higher transference number

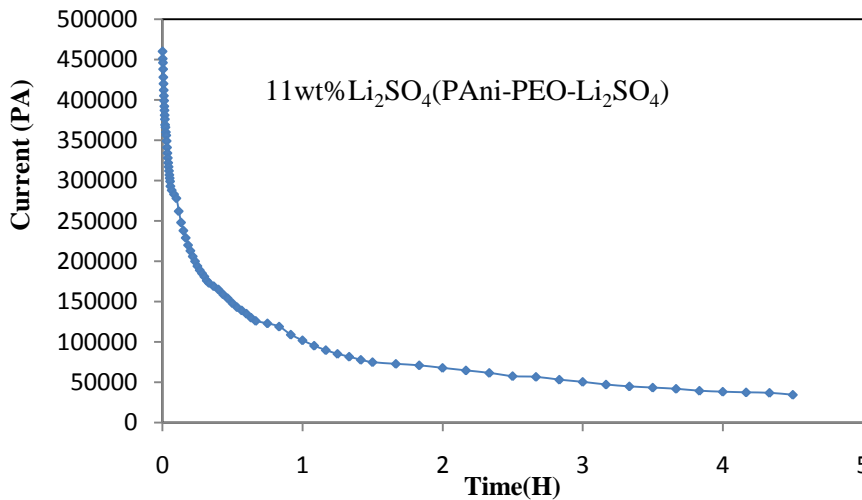




(b)



(d)



(e)

Fig 4.5(a-e) Variation of current as a function of time a) 3 b) 5 c) 7w d) 9 and e) 11wt% of Li_2SO_4 (PAni-PEO- Li_2SO_4) blend.

Table 4.4: Ionic transference number for the PAni-PEO- Li_2SO_4 blend.

wt % of Li_2SO_4 for (PAni-PEO- Li_2SO_4) blend.	Ionic transference number.	Electronic transference number.
	t_{ion}	t_{elec}
3	0.903	0.096
5	0.968	0.026
7	0.974	0.031
9	0.951	0.049
11	0.925	0.075

E. DC conductivity:

The variation of dc electrical conductivity with temperature ($\log \sigma Vs \frac{1}{T}$) for 3,5,7,9 & 11w% of Li_2SO_4 (PAni-PEO- Li_2SO_4) composite films in the temperature range 308 to 333 K shown in Fig (4.6). From it is observed that the dc conductivity of PAni-PEO- Li_2SO_4 composite films depends on temperature. The dc electrical conductivity of these films increases with increase in temperature,

indicating negative temperature coefficient (NTC) of resistance. This shows the semiconducting nature of the films. As the temperature increases the polymer become soft and the mobility of main chain segment as well as the rotation of side groups become easier. Thus, at higher temperature more and more dipoles are oriented resulting in the higher equivalent surface charge density. Dc conductivity follows Arrhenius equation

$$\sigma = \sigma_0 \exp\left(-\frac{E_a}{kT}\right) \quad (4.6)$$

Where σ_0 is the pre-exponential factor, E_a is activation energy and k is the Boltzmann's constant. For the present composite films, these plots ($\log\sigma Vs \frac{1}{T}$) show straight

lines with negative slope indicating the temperature dependence of conductivity. Fig 4.7 shows that conductivity increases with increase in wt% of PANi and is maximum for 7 wt% . Hence optimized wt% is 7wt% of Li_2SO_4 .

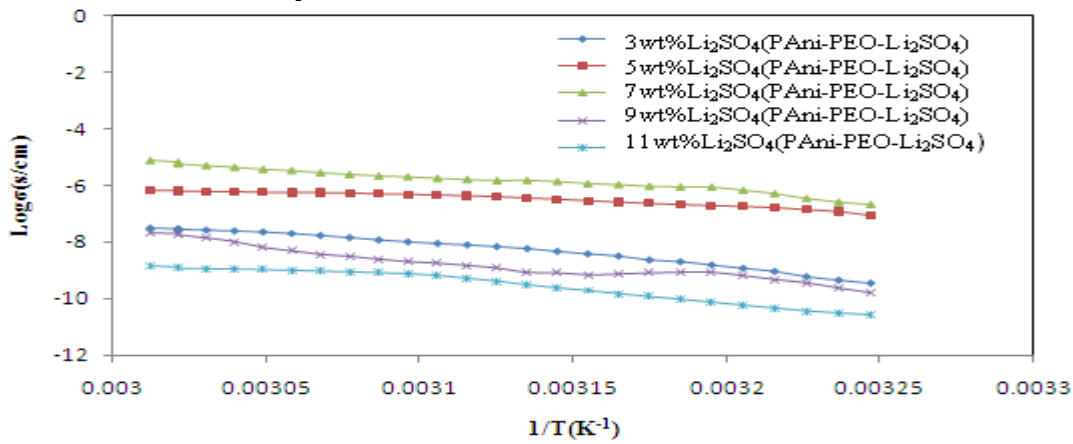


Fig 4.6: Temperature dependence of dc electrical conductivity of PANi-PEO- Li_2SO_4 composite film of different wt %.

The Figure 4.7 shows the conductivity of PANi-PEO- Li_2SO_4 blend with different concentrations and with the addition of lithium salt (Li_2SO_4). The ionic conductivity of the polymer film is increase. The maximum conductivity is achieved at the addition of 7 wt% of Li_2SO_4 gave the conductivity value of $1.96152 \times 10^{-6} Scm^{-1}$. Further increase of Li_2SO_4 causes the conductivity decrease due to the higher salt

concentration, the conductivity decrease may be due to the increasing influence of the ion pairs, ion triplets, and higher ion aggregations, which reduces the overall mobility and degree of freedom. The number of effective charge carriers that transit between anode and cathode are relatively reduced, Mac Callum et al [13].

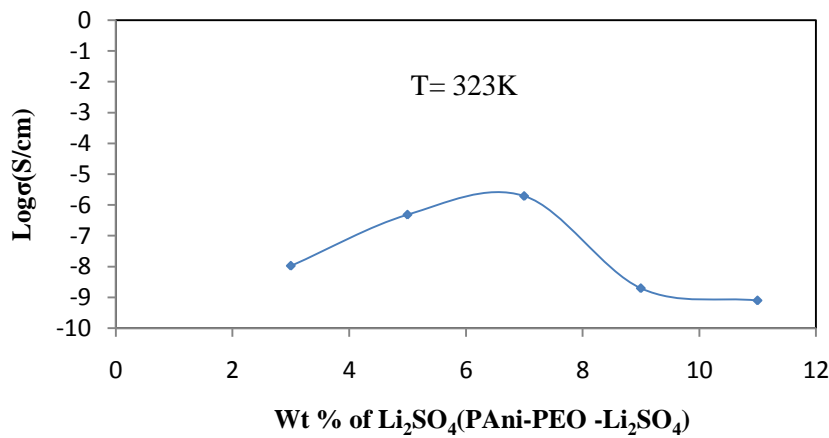


Fig4.7: Variation of $Log\sigma$ (S/cm) with Li_2SO_4 wt% concentration for PANi-PEO- Li_2SO_4 composite at 323K.

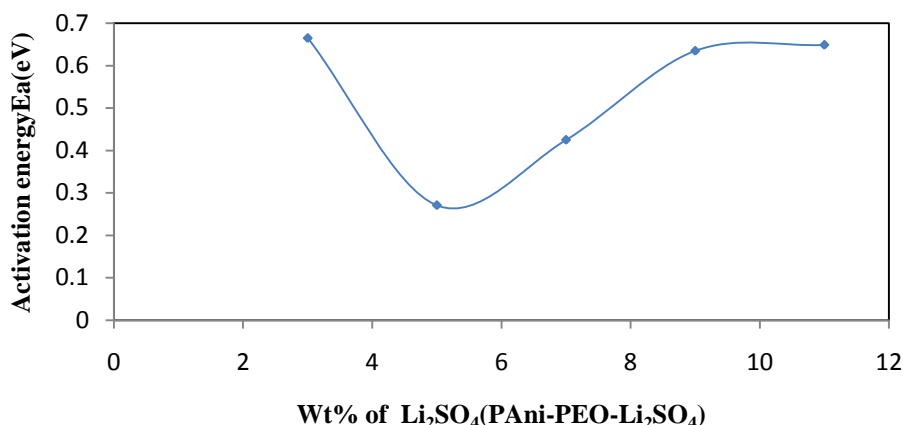


Fig 4.8: Variation of activation energy for D.C. electrical conductivity with Li₂SO₄wt% concentration for PANi-PEO- Li₂SO₄ composite.

At high temperature, the activation energy of dipole segmental processes decreases due to disturbance of the cooperative movement of segments. This explains the decrease of activation energy with increase in temperature . Figure 4.8 shows the variation of activation energy with concentration of Li₂SO₄, the values of activation energy and pre-exponential factor have been calculated from the

Arrhenius plot using $\sigma = \sigma_0 \exp\left(\frac{-E_a}{kT}\right)$ relation. It is summarized in table.4.5, it can be seen that 7wt % Li₂SO₄ added samples has the higher dc electrical conductivity and lower Ea. Ramesh et al. [14] claimed that the low Ea is due to the amorphous nature of the polymer electrolytes that facilitate the fast Li⁺ ion motion in the polymer network

Table 4.5:Activation energy and pre-exponential factor for the PANi-PEO-Li₂SO₄ blend.

wt % of Li ₂ SO ₄ in PANi-PEO-Li ₂ SO ₄ blend	Activation energy, E _a (eV)	pre-exponential factor, σ ₀
3	0.664	1.479x10 ¹⁷
5	0.270	7.780x10 ³
7	0.424	2.630x10 ¹⁰
9	0.634	3.235x10 ¹⁵
11	0.648	1.905x10 ¹⁵

F.Impedance spectroscopy:

The electrical impedance of the conducting composites can give information on the behavior of these materials in the alternating field at different frequencies. The impedance spectra are usually drawn using Z'' vs Z' to yield the Cole-

Cole plot. Figure 4.9 (a-c) shows that the complex impedance plots (Z'' vs Z') of PANi-PEO-Li₂SO₄ blend with (5,7,9) wt% at different temperatures, which corresponding to the properties of bulk material. A beautiful shift in the peaks is observed for decreasing temperatures.

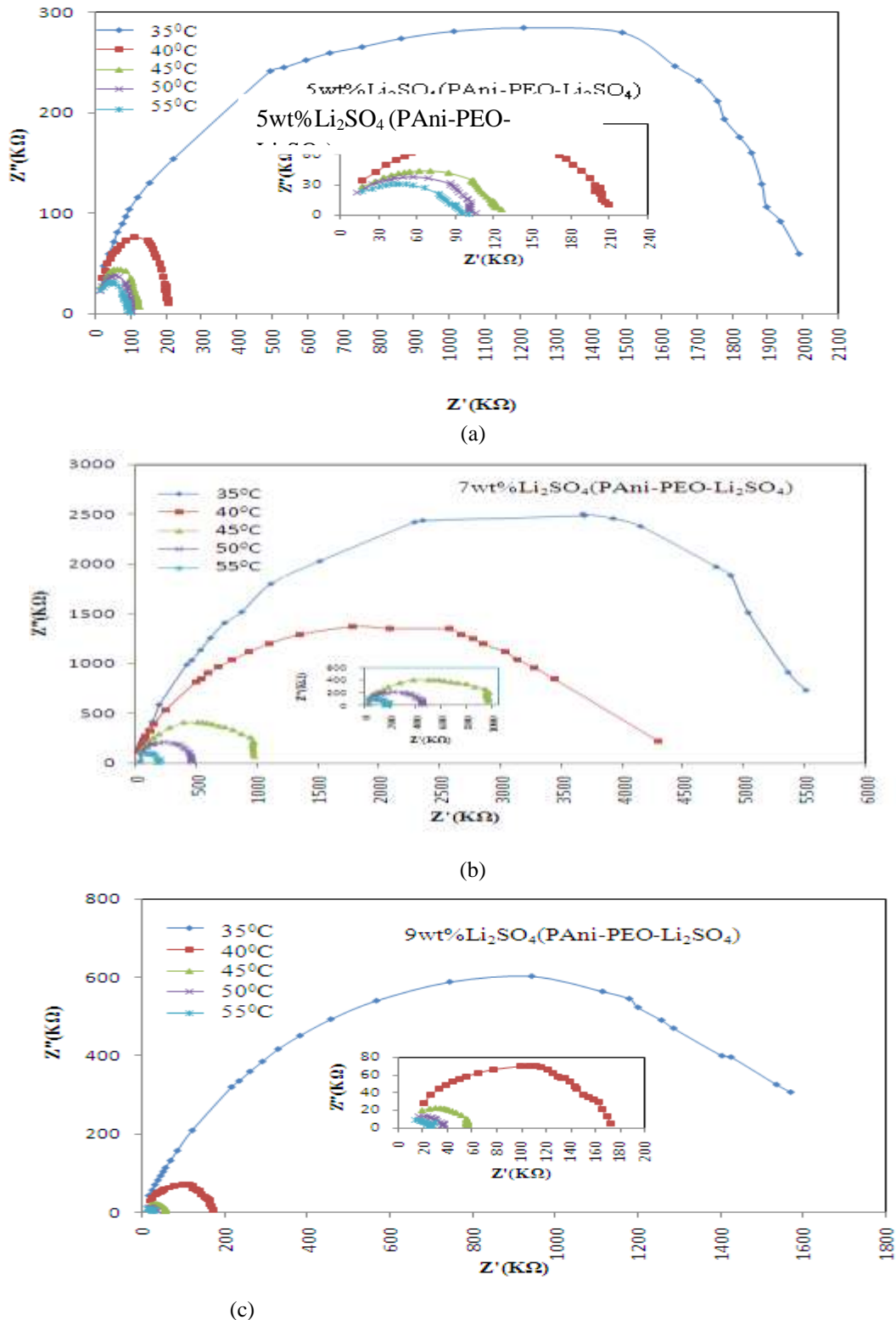


Fig 4.9: Complex impedance spectra of PANi-PEO- Li₂SO₄blend a) 5 b) 7 c) 9wt% at different temperatures.

The inset of Fig.4.9 (a-c) represents the enlarged view of Cole–Cole plot corresponding to the temperature of 40-55°C, 45-55°C, and 40-55°C respectively. It can be seen that the single semi- circle has been observed at all the measuring temperatures. The semi-circles in the higher frequency region correspond to the parallel combination of bulk resistance R_b and bulk capacitance C_b . The

capacitance values were calculated for all the temperatures using the relation $2\pi\omega R_b C_b = 1$ given in table 4.6. These obtained values are in the order of Pico Farads, which reveals that the conduction process is through the bulk of the material [15]. From the figure it is seen that the centre of the semi-circle is found to be depressed below the real axis, which indicates that the relaxation of ions are

non-Debye in nature [16]. The radius of the semi-circle decreases with increase in temperature, which is due to the decrease in bulk resistance, i.e., increase in conductivity. This negative temperature coefficient of resistance

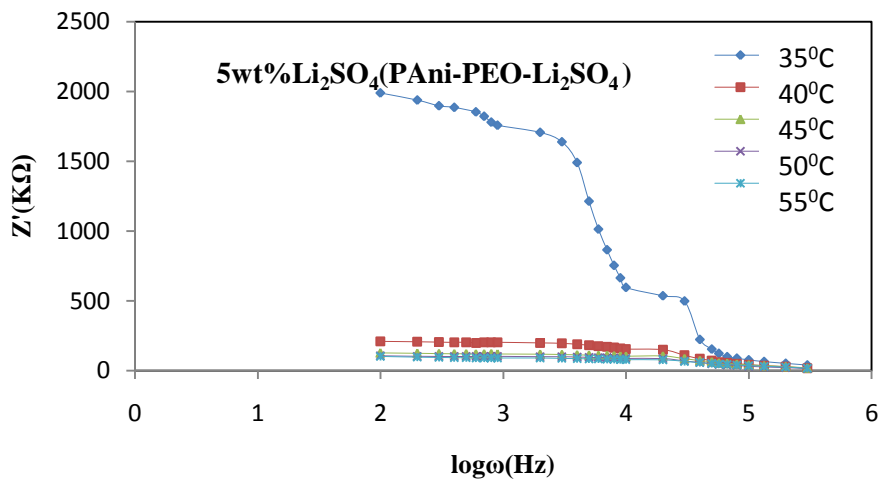
(NTCR) is a typical behavior of semiconducting materials [20]. The reduction in bulk resistance is calculated by intercepting high frequency semi-circles on the X-axis of Fig 4.9.

Table 4.6 Capacitance values of 5,7 and 9wt% Li_2SO_4 for PANi-PEO- Li_2SO_4 blend.

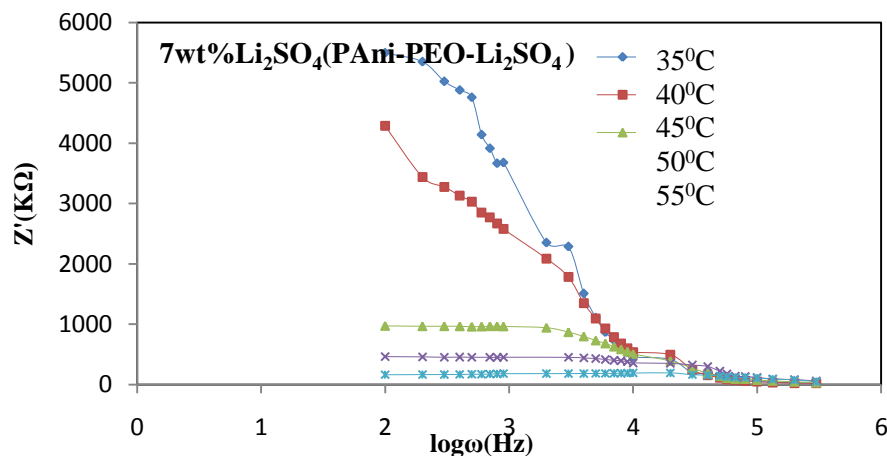
Temperature ($^{\circ}\text{C}$)	(5 wt % of Li_2SO_4 for PANi-PEO- Li_2SO_4 blend)		(7wt % of Li_2SO_4 for PANi-PEO- Li_2SO_4 blend)		(9Wt % of Li_2SO_4 for PANi-PEO- Li_2SO_4 blend)	
	Capacitance (pF)	Bulk Resistance ($\text{K}\Omega$)	Capacitance (pF)	Bulk Resistance ($\text{K}\Omega$)	Capacitance (pF)	Bulk Resistance ($\text{K}\Omega$)
35	25.80	2050	38.55	5900	93.66	1700
40	36.26	219.56	17.69	4500	88.95	179
45	41.46	128	14.34	1110	26.98	59
50	49.14	108	16.76	475	21.00	37.9
55	30.60	104.07	9.56	208	29.48	27

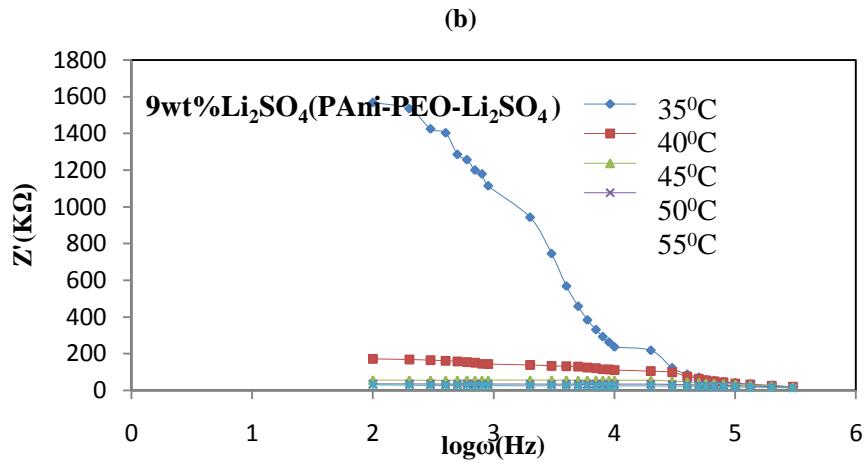
Figure 4.10 (a-c) shows the variation in real part of impedance (Z') with frequency at different temperatures. The curve indicates that the real part of impedance (resistance) decreases with rise in frequency, which infers that the conduction process increases with

temperature and frequency. At higher frequencies all the curves merge together for the entire temperature, which attributes the release of space charge as a result of lowering of barrier properties of materials [21].



(a)

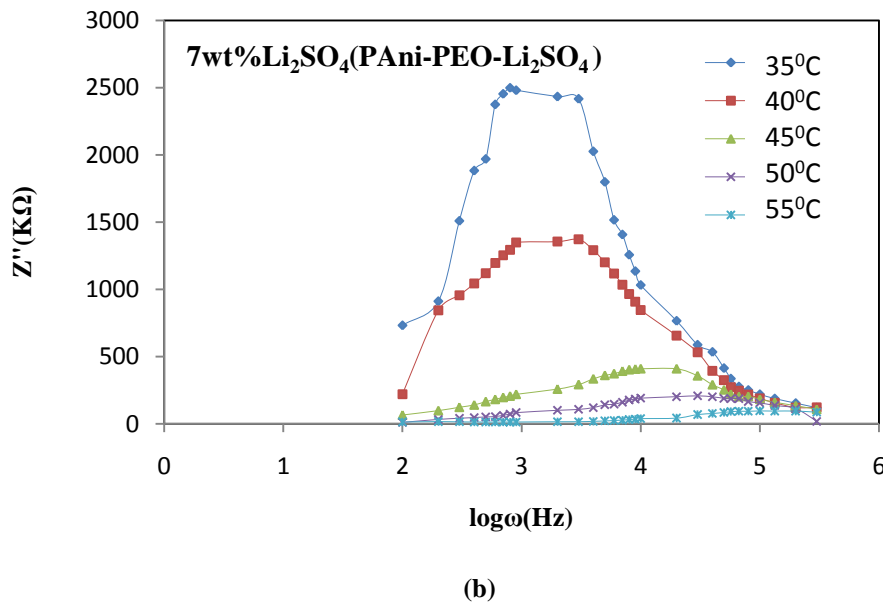
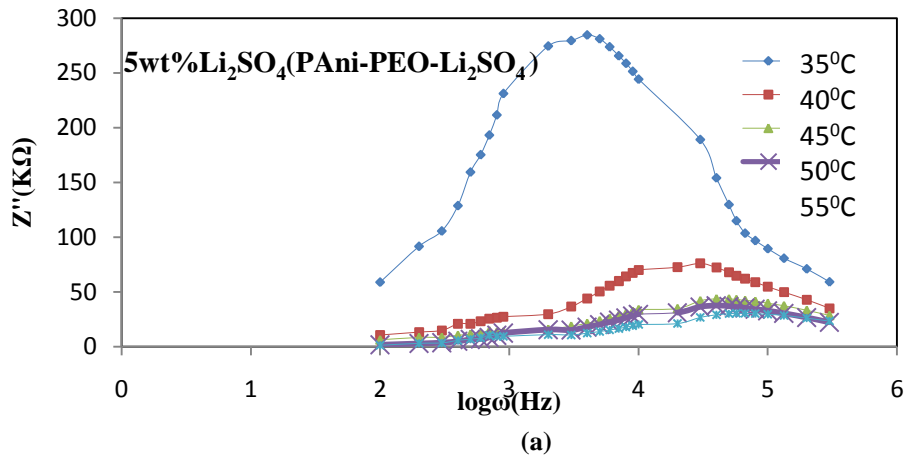


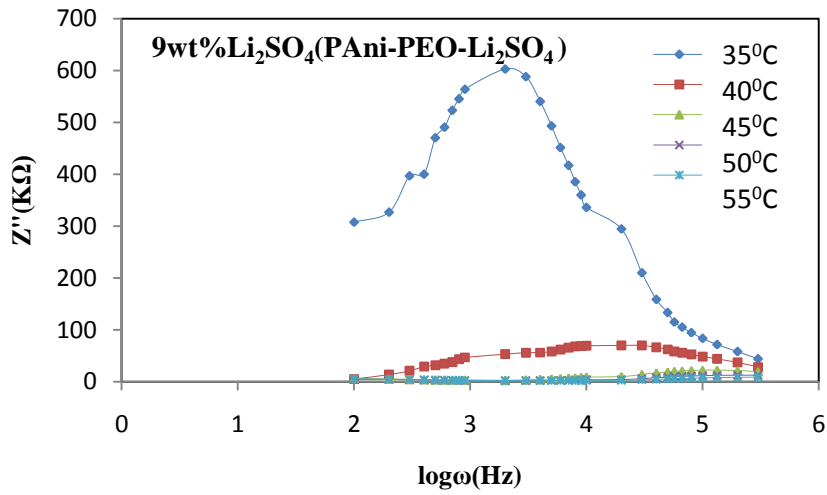


(c) **Fig 4.10: Variation in Z' with frequency at different temperatures of a) 5 b) 7 c) 9wt% of PANi-PEO- Li_2SO_4 blend.**

According to the Maxwell–Wagner model [17], the dielectric material consists of a large number of conductive grains separated by highly resistive grain

boundaries. The voltage applied on the sample drops across the grain boundaries and the space charge is built up at the grain boundaries [18].





(c)

Fig. 4.11: Variation in Z'' with frequency at different temperatures of a) 5 b) 7 c) 9wt% of Li₂SO₄ (PAni-PEO- Li₂SO₄) blend.

Figure 4.11 (a-c) Shows the variation in Z'' as a function of frequency at different temperatures. The relaxation frequency of the most resistive component can be evaluated using this plot. The value of Z'' decreases with increase in temperature and shifts towards the high frequency side. The broadening of the peak with increase in temperature is due to the

temperature dependence of relaxation process in the material. The relaxation process in the material is due to the localized electrons, which are responsible for the conductivity mechanism [19].

Dielectric relaxation energy and relaxation time :

When log f_r versus reciprocal of temperature is plotted a straight line is observed . shown in fig 4.12.

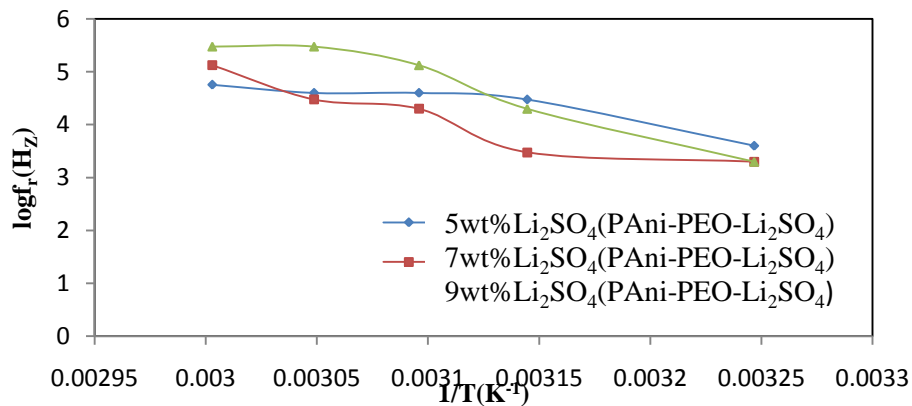


Fig 4.12: Variation of log fr with 1/T for 5, 7 and 9 wt% of Li₂SO₄ (PAni-PEO- Li₂SO₄) blend

The plot is fitted with the relationship

$$f_r = f_{r0} \exp\left(-\frac{\varepsilon}{kT}\right) \quad (4.7)$$

where ε is a Dielectric relaxation energy and K is Boltzmann's, the relaxation time (τ) of the individual PAni-PEO-Li₂SO₄ blend is calculated using the Cole–Cole plots by the relation

$$\tau = 1/2\pi f \quad (4.8)$$

where f is the value of frequency for maximum peak position of Cole–Cole plot. Relaxation energy and Relaxation time is tabulated in the table 4.7

Table 4.7 Relaxation energy and relaxation time for the PAni-PEO-Li₂SO₄ blend.

wt%	Relaxation energy (eV)	Relaxation time(Sec)
5	0.3697	3.31E-19
7	0.7656	2.34E-34

9	0.918	7.76E-41
---	-------	----------

The relaxation times for various wt% of PANi-PEO-Li₂SO₄ blend are as shown in table 4.13. It is observed from

that blend show almost symmetric semicircles indicating the Debye-type relaxation.

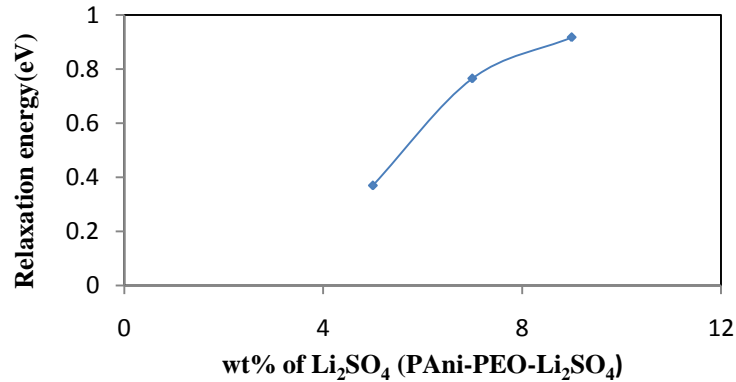


Fig 4.13: Variation of relaxation energy with wt% of Li₂SO₄ (PANi-PEO- Li₂SO₄) composite.

The relaxation energy is calculated from the slope of log f_r Vs 1/T curve. Relaxation energy value are found to be in the range of 0.36 to 0.91 eV. The variation of Relaxation energy (ε) with different wt% of Li₂SO₄ (PANi-PEO-Li₂SO₄) is shown in fig 4.13. The relaxation energy is increase with increase in wt% of Li₂SO₄ in (PANi-PEO-Li₂SO₄).

consist of only one arc which may be taken to mean that the conduction processes have identical time constants. The variation of real axis Z' with log f shows negative temperature coefficient of resistance (NTCR). The variation of imaginary axis Z'' versus log f shows asymmetric peaks at different temperatures that lead to Debye type of relaxation. On the basis of impedance spectra various parameters such as relaxation time, bulk resistance, bulk capacitance, dielectric activation energy etc. are calculated.

V. CONCLUSION:

The SEM-EDX study in case of PANi-PEO films doped with Li₂SO₄ predicts the presence of dopant Lithium in the films. From the SEM of PANi-PEO-Li₂SO₄ blend it was observed "sponge-like" appearance and shows a homogeneous surface, with uniformly distributed particles. It shows amorphous nature. FT-IR identifies the presence of certain functional groups of molecule. Also one can use the unique collection of absorption band to confirm the identity of pure compound or to detect the presence of specific impurities. From the IR spectroscopy, it was noticed that, conductive blends was formed. And the corresponding peak observed in all four series show PANi, PEO and lithium peaks. From the TG/DTA, it is observed that PANi-PEO samples with doped Li₂SO₄ gives one step degradation in which weight loss is in the range 95.5 to 97.32 % when heated up to 700K.

Transference numbers of PANi-PEO-Li₂SO₄ composite films were found to be nearer to 0.9 which suggests the presence of ionic conduction.

Temperature dependant conductivity of PANi-PEO films doped with Li₂SO₄ follows Arrhenius nature. On the basis of dc conductivity, dc parameters such as activation energy and pre-exponential factors are calculated and noted. The impedance spectra of PANi-PEO-Li₂SO₄ blend was found to

VI. ACKNOWLEDGEMENT

It is great sense of privilege to have this opportunity to acknowledge with a feeling of deep gratitude the prompt and excellent guidance given by my guide **Dr. S. S. Yawale**, Director, of Govt. Vidarbha Institute of Science and Humanities, Amravati (M.S.) who suggest this project and has been a constant source of inspiration and encouragement in all stages of the present work right from conceptualization to its final completion. I gratefully acknowledge her patience, constructive criticism and generous treatment throughout the progress of my research work. With immense pleasure I thank **Dr. S. P. Yawale**, Head, Department of Physics, Govt. Vidarbha Institute of Science and Humanities, Amravati (M.S.) for his keen interest and valuable guidance during course of this work. I found in his, a guide who is always there to help you out not only in scientific problem but personal as well. I am deeply indebted to his for timely help. Also I am grateful to the **Dr. S. P. Yawale** for permitting me to carry out this research work in the materials research laboratory of the Institute. This work would never have been finished timely without endless loving support of my husband. I am thankful to all my friends for their cooperation during this work. Last but not

the least, I thank them those who have directly or indirectly helped me during my work.

REFERANCES:

- [1] Sreejith V. J. *Polymer Science and Engg Chemical Engg Division NCL, Pune*, 5(2004).
- [2] Xiang-Wu Zhang et al. Center for Electrochemical Systems and Hydrogen Research, Texas Engineering Experiment Station, *Texas A & M University, College Station, TX, USA*, 31 May(2002)77843-3402
- [3] Sanchez, Chantal Ince, J. *Composites Science and Technology* **69** (2009) 1310–1318.
- [4] L. Bohaty, P. Becker, H. J. Eichler, K. Udaya, *Laser Physics*, **15**(11), (2005) 1509– 1522.
- [5] V.DaryaRadziuk and HelmuthMöhwald, *Polymers* **3**(2011), 674-692.
- [6] J. Prokes, et.al., *Polym. Degrad. Stab.*, **78**(2002)393.
- [7] A. J. Epstein. et. al., *Synth. Met.*, **16**(1986) 305.
- [8] Z.J Ping, *Chem. Soc. Faraday. Trans.*, **92** (1996) 3063.
- [9] S. Quillard, et. al., *Synth. Met.*, **84** (1997) 805.
- [10] G. Socrates, *Infrared Characteristic Group Frequencies*. Wiley, Chichester (1980).
- [11] Z. Shen, P. George, Yi-Bing Cheng, *Polymer* **43** (2002)4251-4260.
- [12] T. K. Vishnuvardhan, V. R. Kulkarni, C. Basavaraja, S. C. Raghavendra, *Bull. Mater. Sci.* **29** (1) (2006) 77-83.
- [13] J. R. Mac Callum, A. S. Tomlin, and C. A. Vincent, *European Polymer J.*, **22** (1986) 787.
- [14] S. Ramesh and A. K. Arof, *Mat. Scn. & Eng. B-solid state Mat. for Advanced Technology*, **85** (2001) 11.
- [15] R. Amin, C. Lin, J. Peng, K. Weichert, T. Acarturk, U. Starke, J. Maier, *Adv. Func. Mater.* **19** (2009)1697.
- [16] R. Ranjan, R. Kumar, B. Behera, R. N. P. Choudhary, *Physica B* **404** (2009)3709.
- [17] C. Koops, *Phys. Rev* **83** (1951) 121.
- [18] A. M. Abo El Ata, S. M. Attia, T. M. Meaz, *Solid State Sci.* **6** (2004) 61.
- [19] B. Behera, P. Nayak, R. N. P. Choudhary, *Curr. Appl. Phys.*, **9** (2009) 2010.
- [20] S. Quillard, G. Louarn, S. Lefrant, A. G. MacDiarmid, Vibrational analysis of polyaniline: a comparative study of leucoemeraldine, emeraldine, and pernigraniline bases, *Phys. Rev. B* **50** (1994) 12496–12508.
- [21] Liliana Hechavarría, Hailin Hu*, Marina E. Rinco'n, *J. Thin Solid Films* **441** (2003) 56–62.